Colloids and Surfaces B: Biointerfaces 113 (2014) 43–50

Contents lists available at ScienceDirect

Colloids and Surfaces B: Biointerfaces

journal homepage: www.elsevier.com/locate/colsurfb

Paclitaxel-loaded PCL–TPGS nanoparticles: *In vitro* and *in vivo* performance compared with Abraxane®

Ezequiel Bernabeu[a], Gustavo Helguera[a,b], Maria J. Legaspi[a], Lorena Gonzalez[b,c], Christian Hocht[d], Carlos Taira[b,d], Diego A. Chiappetta[a,b,*]

[a] Department of Pharmaceutical Technology, Faculty of Pharmacy and Biochemistry, University of Buenos Aires, Argentina
[b] National Science Research Council (CONICET), Faculty of Pharmacy and Biochemistry, University of Buenos Aires, Argentina
[c] Department of Biological Chemistry, Faculty of Pharmacy and Biochemistry, University of Buenos Aires, Argentina
[d] Department of Pharmacology, Faculty of Pharmacy and Biochemistry, University of Buenos Aires, Argentina

ARTICLE INFO

Article history:
Received 30 January 2013
Received in revised form 17 June 2013
Accepted 16 July 2013
Available online xxx

Keywords:
Polymeric nanoparticles
PCL–TPGS
Paclitaxel
In vitro anti-tumoral activity
In vivo pharmacokinetic studies

ABSTRACT

The purpose of this work was to develop Cremophor® EL-free nanoparticles (NPs) loaded with Paclitaxel (PTX) in order to improve the drug i.v. pharmacokinetic profile and to evaluate its activity against commercially available formulations such as Taxol® and Abraxane®. PTX-loaded poly(ε-caprolactone)–alpha tocopheryl polyethylene glycol 1000 succinate (PCL–TPGS) NPs were prepared using three different techniques: (i) by nanoprecipitation (NPr-method), (ii) by emulsion-solvent evaporation homogenized with an Ultra-Turrax® (UT-method) and (iii) by emulsion-solvent evaporation homogenized with an ultrasonicator (US-method). The NPs prepared by US-method showed the smallest size and the highest drug content. The NPs exhibited a slow and continuous release of PTX. The *in vitro* anti-tumoral activity was assessed using two human breast cancer cell lines (MCF-7 and MDA-MB-231) with the WTS assay. Cytotoxicity studies with both cell lines showed that PTX-loaded PCL–TPGS NPs exhibited better anti-cancer activity compared to PTX solution and the commercial formulation Abraxane® at different concentrations. Importantly, in the case of triple negative MDA-MB-231 breast cancer cells, the IC_{50} value for PTX-loaded PCL–TPGS NPs was 7.8 times lower than Abraxane®. Finally, *in vivo* studies demonstrated that PTX-loaded PCL–TPGS NPs exhibited longer systemic circulation time and slower plasma elimination rate than Taxol® and Abraxane®. Therefore, the novel NPs investigated might be an alternative nanotechnological platform for PTX delivery system in cancer chemotherapy.

1. Introduction

In the last World Health Organization (WHO) report, cancer is a leading cause of death worldwide. Approximately 70% of deaths occur in low- and middle-income countries [1]. Breast cancer is now the most frequent cancer in women both in the developed and the developing world [2]. The largest number of cases occurs in low- and middle-income countries where breast cancer is diagnosed in very late stages [3]. Nowadays, the main practice for breast cancer treatment is surgery followed by radiotherapy and/or chemotherapy. Despite advances on treatment, approximately one third of patients will eventually develop metastatic breast cancer. They have bad prognosis with a median survival time between 18 and 24 months [4]. The use of the adjuvant chemotherapy is increasingly important in the breast cancer treatment [5]. Therefore, is paramount developing novel anticancer drug formulations to improve the drug biodistribution and the therapeutic efficacy [6].

Paclitaxel (PTX) is one of the most effective antineoplastic drugs used for the treatment of breast and ovarian cancer [7]. It is a hydrophobic drug with poor solubility in water (0.3–0.5 μg/mL) [7–9]; for this reason, it is commonly formulated as Taxol®, a market formulation composed by a mixture of Cremophor EL® and dehydrated alcohol (1:1, v/v) [7]. This vehicle is associated with a variety of side effects such as hypersensitivity, nephrotoxicity and neurotoxicity, attributable mainly to Cremophor EL [10]. This solubilizing agent also causes vasodilation, labored breathing, lethargy and hypotension [11]. For this reason, premedication must be given to patients in order to prevent hypersensitivity reactions. Moreover, since cremophor solubilizes the plasticizers, Taxol® requires the use of non-plasticized solution containers such as diethylhexylpthalate in the polyvinylchloride infusion bags/sets [12].

Nanoparticulate systems have been studied for several decades offering an advantageous alternative to the use of toxic excipients

* Corresponding author at: Department of Pharmaceutical Technology, Faculty of Pharmacy and Biochemistry, University of Buenos Aires, 956 Junín Street, 6th Floor, Buenos Aires CP1113, Argentina. Tel.: +54 11 4964 8271; fax: +54 11 4964 8271.
E-mail address: diegochiappetta@yahoo.com.ar (D.A. Chiappetta).

0927-7765/$ – see front matter © 2013 Elsevier B.V. All rights reserved.
http://dx.doi.org/10.1016/j.colsurfb.2013.07.036

to improve drug solubility and favor a sustained drug release. A very important point in the chemotherapy is that drug-loaded nanoparticles (NPs) can escape from the vasculature through the leaky endothelium overlying the tumor and then accumulate preferentially in many types of solid tumors by the phenomenon known as Enhanced Permeability and Retention (EPR) effect [13]. Various PTX formulations such as liposomes [14,15], solid lipid nanoparticles [16,17], polymeric NPs [18], polymeric micelles [19,20] and drug conjugates [21,22] have been examined to achieved certain improvements in PTX solubility. Few years ago, the Food and Drug Administration (FDA) has approved a Cremophor® free formulation of albumin-bound PTX NPs (Abraxane®) for recurrent metastatic breast cancer [23]. In this formulation, PTX is formulated within albumin particles to retain the pharmacotherapeutic benefits of PTX and eliminate the adverse effects associated with Cremophor® [24]. However, it has been demonstrated that Abraxane® shows a rapid elimination of PTX from the blood circulation and do not improve the pharmacokinetics of PTX (Taxol®) [24]. Moreover, it is a high-cost formulation which might not be available for every patient, especially for those living in low- and middle-income countries.

Surface modification of NPs allows longer blood-circulation and favors its preferential accumulation in solid tumors by EPR effect. D-α-Tocopheryl polyethylene glycol 1000 succinate (TPGS) is a water-soluble derivative of natural vitamin E and polyethylene glycol (PEG) 1000. TPGS has been used as solubilizer and absorption enhancer in some drug delivery formulations. Also, TPGS inhibits P-gp-mediated multidrug resistance in tumor cells, and thus enhance drug permeation and increases the oral bioavailability of anticancer drugs [25]. It was found that TPGS could also effectively inhibit the growth of human lung carcinoma cells *in vitro* and *in vivo* [26].

In this work, we have synthesized a poly(ε-caprolactone)–tocopheryl polyethylene-glycol-succinate (PCL–TPGS) copolymer by ring opening polymerization with an hydrophobic–hydrophilic balance adequate for the NP formulation. PCL is an important synthetic biomedical material with controlled biodegradability, great biocompatibility and low cost. It is used in some drug delivery systems approved by FDA and European Medicines Agency (EMA) [27]. TPGS presents the PEG repulsive properties providing higher stability of the NPs in biological fluids [25]. In order to confirm the advantageous features of this novel PTX-loaded nano-sized platform in anticancer therapy, we have evaluated its *in vitro* cytotoxicity against two human breast cancer cell lines (MCF-7 and multidrug resistant MDA-MB-231). In addition, this novel NP formulation was evaluated *in vivo versus* two available commercial formulations (Taxol® and Abraxane®).

2. Experimental

2.1. Materials

Paclitaxel (PTX) of purity 99.9% was purchased from Rhenochem AG (Basel, Switzerland), D-α-tocopheryl polyethylene-glycol (PEG) 1000 succinate (TPGS, M_W ~1513 g/mol) was from Eastman Chemical Company (Kingsport, TN, USA). ε-Caprolactone (CL, M_W 114.14 g/mol), tin(II) 2-ethylhexanoate (SnOct, M_W 405.12 g/mol) and Cremophor EL® were purchased from Sigma–Aldrich (St. Louis, MO, USA). Tetrazolium compound [3-(4,5-dimethylthiazol-2-yl)-5-(3-carboxymethoxyphenyl)-2-(4-sulfophenyl)-2H-tetrazolium], inner salt (MTS) and phenazine methosulfate (PMS) were purchased from Promega Corporation (Madison, WI, USA). Clinical formulation Abraxane® was supplied by Aventis Pharmaceuticals, USA. All solvents such as acetone, acetonitrile and dichloromethane (DCM) were of analytical or high performance liquid chromatography (HPLC) grade and were used following the manufacturer's instructions.

2.2. Synthesis of PCL–TPGS copolymer

The copolymer synthesis was performed in a household microwave oven (Whirlpool®, WMD20SB, microwave frequency 2450 MHz, potency 800 W, Argentina) with ten power levels. Conventional microwave ovens graduate the irradiation power by controlling on/off cycles of the magnetron (pulsed irradiation) [28]. The potency in this microwave oven is 800 W and the duration of the on/off period is modified according to the power level used. The oven was adapted in the laboratory to enable the connection of a condenser. PCL–TPGS copolymer was synthesized by the ring opening polymerization of CL by TPGS in presence of SnOct. Briefly, TPGS (3.0 g) was poured into a 250 mL round-bottom flask and dried. Then, CL (20.0 g) and SnOct (0.04 g) were added, and the round-bottom flask was placed in the center of the microwave oven and connected to the condenser. The reaction mixture was exposed to microwave radiation for: (i) 1 min at power 5, (ii) 2 min at power 3, (iii) 2 min at power 3, (iv) 5 min at power 3 and (v) 1 min at power 5. The total reaction time was 11 min, under reflux. Then, the crude was dissolved in dichloromethane (50 mL) and precipitated in methanol (500 mL) to isolate the product. The product obtained was recuperated by filtration, washed several times with methanol, dried until constant weight at room temperature and stored at 4 °C until use. Finally, a white to yellowish solid was obtained.

2.3. Characterization of PCL–TPGS copolymer

Proton nuclear magnetic resonance (^{1}H NMR) spectra were obtained from deuterated chloroform (Sigma) solutions at room temperature on a Bruker MSL300 spectrometer (Karlsruhe, Germany), at 300 MHz. The hydrophobic/hydrophilic balance, as represented by the CL/EO molar ratio, and the number-average molecular weight (M_n) of the copolymer were calculated by the ratio of the integration area of the peaks of PCL methylene protons (4.07 ppm) and PEG methylene protons (3.65 ppm) of PEG part of TPGS.

Fourier transform infrared (FT-IR) spectra were recorded in an FT-IR Spectrophotometer (Nicolet 380 FT-IR Spectrometer, Avatar Combination Kit, Smart Multi-Bounce HATR with ZnSe crystal 45° reflectance, Thermo Scientific, USA).

2.4. Preparation of PTX-loaded NPs

PTX-loaded NPs were prepared using PCL–TPGS by three different methods: (i) nanoprecipitation (NPr-method); (ii) emulsion-solvent evaporation homogenized with an Ultra-Turrax® (UT-method); and (iii) emulsion-solvent evaporation using an ultrasonicator as homogenizer (US-method).

2.4.1. NPr-method

PCL–TPGS (70 mg total weight) were poured into acetone (5 mL) and stirred until complete dissolution. Then, PTX (7 mg) was added and thoroughly mixed. This organic solution was drop-wise added to 20 mL distilled water containing TPGS (0.03%, w/v) under moderate magnetic stirring at room temperature. The resulting suspension was stirred overnight at room temperature to allow the complete evaporation of the organic solvent and favor the precipitation of the NPs. Then, the dispersion was filtered under vacuum through filter paper (VWR® Grade 410 Filter Paper, Qualitative, 1 μm, Darmstadt, Germany) and centrifuged for 1 h at 7500 rpm. The supernatant was discarded and the pellet was resuspended in water. Finally, samples were frozen at −20 °C and lyophilized (freeze-dryer FIC-L05, FIC, Scientific Instrumental Manufacturing, Argentina) for 48 h. Products were stored at 4 °C until use. Blank NPs were used as controls.

2.4.2. UT-method

In this case, first we prepared a stock solution of PTX in dichloromethane (1.4 mg/mL). Then, PCL–TPGS (42 mg total weight) was added to a 3 mL of PTX stock solution and vortexed until complete dissolution. This solution was poured slowly and carefully into distilled water (100 mL) containing TPGS (0.03%, w/v) and emulsified by homogenization with a T25 Basic Ultra-Turrax (IKA®-Werke GmbH & Co. KG, Germany) at 24,000 rpm for 5 min. The resulting emulsion o/w was stirred under magnetic stirring overnight at room temperature. Then, the sample was vacuum-filtered through filter paper (VWR® Grade 410 Filter Paper, Qualitative, 1 μm) and the suspension was frozen at −20 °C and lyophilized for 48 h (see above). Blank NPs were used as controls.

2.4.3. US-method

The copolymer and drug solution was prepared as described previously. This solution was poured carefully into distilled water (100 mL) containing TPGS (0.03%, w/v) and emulsified by sonication using a probe sonicator (Q700 ultrasonic liquid processor, Qsonica, Newton, CT, USA) at an output of 50 W for 60 s. Then, the sample was treated as in the UT-method to obtain the NPs. Blank NPs were used as controls.

2.5. Determination of PTX content in NPs

PTX concentration in the NPs was determined by high performance liquid chromatography (HPLC) Instrument (Shimadzu SCL-10A, Japan) equipped with a plus autosampler (Shimadzu SIL-10A, Japan) and UV-detector (Shimadzu SPD-10A, Japan). Chromatographic separations were performed on a reversed phase C18 column (4.6 mm × 250 mm, 5 μm, Fluophase PFP, Thermo, USA). Acetonitrile/water (50/50, v/v) was used as eluent at a flow rate of 1 mL/min. Detection wavelength was 227 nm. Sample solution was injected at a volume of 20 μl. The HPLC was calibrated with standard solutions of 5–100 μg/mL of PTX dissolved in acetonitrile (correlation coefficient of $R^2 = 0.996$). The limit of quantification was 0.3 ng/mL. The coefficients of variation (CV) were all within 4.3%. NPs were dissolved in acetonitrile and vigorously vortexed to get a clear solution. Finally, drug loading (DL) and efficiency encapsulation (EE) of drug-loaded NPs were calculated according to Eqs. (1) and (2):

$$\mathrm{DL}(\%) = \left(\frac{\text{Weight of PTX in the NPs}}{\text{Total weight of NPs}}\right) \times 100 \quad (1)$$

$$\mathrm{EE}(\%) = \left(\frac{\text{Weight of PTX in NPs}}{\text{Initial weight of PTX used}}\right) \times 100 \quad (2)$$

2.6. Characterization of the nanoparticles

The average particle size and size polydispersity of the PTX-loaded NPs were determined by Dynamic Light Scattering (DLS, Zetasizer Nano-Zs, Malvern Instruments, UK) provided with a He–Ne (633 nm) laser and a digital correlator ZEN3600. Measurements were conducted at a scattering angle of $\theta = 173^\circ$ to the incident beam. Samples were equilibrated at 25 °C for at least 3 min prior to the analysis. Previously, the instrument was calibrated with standard latex nanoparticles provided by Malvern Instruments, UK. Zeta potential was measured using the same instrument at 25 °C. Experimental values were the average of three different formulations.

The morphology of lyophilized PTX-loaded NPs was characterized by means of field emission gun scanning electron microscopy (FEG-SEM, Zeiss Supra 40 TM apparatus Gemini column, Germany) operating at an accelerating voltage of 3.0 kV. NPs were coated with a thin layer of gold (thickness of 5–10 nm) by sputtering.

2.7. Differential scanning calorimetry (DSC)

The physical state of PTX loaded in PCL–TPGS NPs was investigated by differential scanning calorimetry (DSC, Mettler Toledo TA-400 Differential Scanning Calorimeter, USA). Samples (4–7 mg) of pure PTX, blank NPs (US-method), physical mixture of PTX:blank NPs (proportion 5:95, respectively) and PTX-loaded NPs (US-method) were sealed in 40 μl Al crucible-pans (Mettler ME-27331, Switzerland) and heated in a simple heating temperature ramp between 25 and 300 °C (10 °C/min) under dry nitrogen atmosphere. The different thermal transitions were analyzed.

2.8. In vitro PTX release

In vitro release of PTX from NPs prepared by NPr- and US-method were performed using the dialysis method over 168 h. NPs containing 1 mg of PTX were dispersed in phosphate buffer USP 30 (pH 7.4, 3 mL) containing 0.5% (v/v) of polysorbate 80. The resulting suspension was placed into a dialysis bag (regenerated cellulose dialysis membranes; molecular weight cut off of 3500 g/mol; Spectra/Por® 3 nominal flat width of 45 mm, diameter of 29 mm and volume/length ratio of 6.4 mL/cm; Spectrum Laboratories, Inc., Rancho Dominguez, CA, USA), sealed, and placed in a Falcon® conical tube (15 mL) containing the release medium (PBS, pH 7.4 containing 0.5% (v/v) of polysorbate 80, 12 mL). Polysorbate 80 was added to increase the intrinsic solubility of PTX in the release medium and to ensure sink conditions [29]; as already mentioned, PTX is poorly water soluble. Then, each Falcon® conical tube was placed in an orbital water bath shaking at 40 rpm at 37 °C. At every time intervals (1, 2, 4, 6, 8, 24, 48, 72, 96, 120, 144 and 168 h), 12 mL aliquots were withdrawn and replaced with an equal volume of fresh medium pre-heated at 37 °C. The released PTX amounts were quantified by HPLC as described above (with minor modifications) with correction for the volume replacement. Assays were carried out in triplicate and the results are expressed as mean ± S.D. The analysis of the release kinetics and the fitting to different release models was conducted with Microsoft® Excel 2007 for order zero, order one and Higuchi model, and with SigmaPlot® 2001 software for Korsmeyer–Peppas model. The last one is a simple, semi-empirical model generally used to analyze release data of different pharmaceutical dosage forms when the release mechanism is not well known or when more than one type of release phenomena could be involved. The Korsmeyer–Peppas model is represented by Eq. (3) [30]:

$$\frac{M_t}{M_\infty} = kxt^n \quad (3)$$

where M_t/M_∞ is the fractional release of the drug at time t; k is a constant that incorporates structural and geometric characteristics of the drug dosage form; and n is the release exponent. In this model, only the release fraction curves with a value $M_t/M_\infty \leq 0.6$ were used.

2.9. In vitro cytotoxicity

MCF-7 and MDA-MB 231 human breast cancer cell lines were obtained from the American Type Culture Collection (ATCC) (Rockville, MD, USA). Cells were maintained in Dulbecco's minimum essential medium (DMEM®) supplemented with 10% fetal bovine serum (FBS), 50 μg/mL gentamycine (Invitrogen, Argentina) and 2 mM L-glutamine (Invitrogen, Argentina). The cells were maintained in an incubator at 37 °C in a humidified atmosphere of 5% CO_2. For *in vitro* cytotoxicity assays, cells were seeded in clear 96-well plates (Corning Costar, Fisher Scientific, USA) at a density of 5000 cells/well and incubated 24 h to allow cell attachment. The cells were then incubated with PTX, Abraxane®, Blank NPs and

PTX-loaded NPs for 48 h. The final concentration of PTX was in the range of 0.025 and 100 μg/mL. The blank culture medium was used as a blank control. After the incubation period, the medium was removed, the wells were washed with PBS and fresh medium was added. Finally, the water soluble tetrazolium (WST) salts solution prepared according to manufactures instructions (CellTiter 96® aqueous non-radioactive cell proliferation assay, Promega) was added and cells were incubated for 2 h. The absorbance at 490 nm was measured using a microplate reader (Biotrak II Plate Reader, Amershan Bioscienes, Piscataway, NJ, USA). Triplicates were run for each treatment. Values were expressed in terms of percent of untreated control cells set as 100%.

2.10. In vivo pharmacokinetic studies

Pharmacokinetics of PTX formulated as Taxol®, Abraxane® and PCL–TPGS NPs were investigated using male Wistar rats weighing 300–350 g. Animal experiments were performed in accordance with the "Principles of laboratory animal care" (NIH publication no. 85-3, revised 1985) and local regulations. Animals were maintained on a 12 h light/dark cycle at 22 ± 2 °C with the air adequately recycled. All animals received a standard rodent diet (Asociación Cooperativas Argentinas, Buenos Aires, Argentina) with the following composition (w/w): 20% proteins, 3% fat, 2% fiber, 6% minerals, and 69% starch and vitamin supplements, containing the same amount of calories. Animals were anesthetized with ether, and the left carotid artery and left femoral vein were cannulated with polyethylene cannulae containing heparinized saline solution (25 U/mL). Cannulae were tunneled under the skin and externalized at the back of the neck. Experiments were performed in freely moving animals 2 h after cannulae placement. The different formulations of PTX used were diluted with saline at a PTX concentration of 6 mg/mL. PTX, at a dose of 6 mg/kg ($n = 5$ for each group) was injected intravenously (i.v.) during 15 s. Blood samples (<300 μl) were collected from the arterial cannulae at different times (0.08, 0.25, 0.5, 1, 2, 4, 6, and 24 h) and collected in polypropylene microcentrifuge tubes. The samples were immediately centrifuged at 9000 rpm for 3 min to isolate the plasma. The collected plasma was stored at −70 °C in an ultra-low temperature freezer (Operon, Kimpo City, Kyeonggi-do, Korea) and subsequently analyzed by HPLC.

To determined PTX concentration, 150 μl acetonitrile was added to 75 μl plasma and vortexed for five min. Then, samples were centrifuged (MiniSpin® plus™, Eppendorf AG, Hamburg, Germany) at 13,000 rpm for 4 min. The supernatant was removed to clean test tubes and 5 μl aliquots were injected into the HPLC for analysis. PTX was quantified by HPLC as described above (Section 2.5) with some modifications. The HPLC separation was performed on a Zorbax Eclipse XDB-C18 analytical column (4.6 mm × 150 mm, particle size 3.5 μm, Agilent Technologies, USA) and C^{18} precolumn of the same packing. The HPLC method was validated for PTX quantification in biological matrix. The limit of detection (LOD) and quantification (LOQ) were 1 ng/mL and 5 ng/mL, respectively. A calibration curve ($y = 8786.7x + 4867.3$, correlation coefficient, $r^2 = 0.995$) was prepared using seven calibration standards (20–50,000 ng/mL). The precision of the assay method was validated by the determination of the intra- and inter-day coefficient of variation (% R.S.D.). All % R.S.D.s were less 10% and the average % R.S.D. was below 2%.

Pharmacokinetic analysis was performed by using the TOPFIT program (version 2.0, Dr. Karl Thomae Gmbh, Schering AG, Gödecke AG, Germany). Non-compartment model was used to fit the data. The following data were calculated: area under the curve (AUC); terminal plasma elimination half-life ($t½$), total body clearance (Cl) and volume of distribution at steady state (V_{ss}).

Statistical analysis was performed using GraphPad Prism version 5.02 for Windows® (GraphPad® Software, San Diego, CA, CA). Pharmacokinetic parameters were log transformed for statistical analysis in order to reduce heterogeneity of the variance, and further compared by one-way analysis of variance and the Bonferroni *post hoc* test. Statistical significance was defined as $p < 0.05$.

3. Results and discussion

3.1. Copolymer synthesis and characterization

The PCL–TPGS copolymer was synthesized by the ring opening polymerization of CL by TPGS in presence of SnOct as catalyst; this catalyst has been approved by the US FDA for use in biomedical devices [31]. The hydroxyl end of TPGS served as macro-initiator to selectively cleave acyl-oxygen chain of CL.

In this case, the conventional thermal synthetic reaction was replaced by a microwave-assisted one. The use of microwave-assisted synthesis has important advantages such as: (i) shorter reaction times; (ii) higher yields; and (iii) the relatively easy scale-up [28]. Reaction time was substantially shorter (11 min) and yields were greater than 80%. This new alternative appears as a very interesting approach for the synthesis of biomaterials for pharmaceutical applications.

The structure of the synthesized PCL–TPGS copolymer was analyzed by ^{1}H NMR in $CDCl_3$. Fig. 1 shows typical ^{1}H NMR spectrums of TPGS and PCL–TPGS copolymer. The peak at 3.65 ppm (Fig. 1A) was assigned to the —CH_2 protons of PEG part of TPGS [32]. The smaller peaks in the aliphatic region belong to various portions of vitamin E tails [33]. The peaks at 4.07, 2.32, 1.61–1.71 and 1.34–1.44 were assigned to —OCH_2, —$COCH_2$, —CH_2 (4H) and —CH_2 (2H) segment of PCL, respectively [34]. The Mn value of PCL–TPGS copolymer was determined to be 31,200 g/mol and it was calculated by using the ratio between the peak areas at 4.07 and 3.65.

The FT-IR spectrum of TPGS showed a carbonyl band at 1725 cm^{-1}. In the spectrum of PCL–TPGS copolymer, we note a strong band of ester carbonyl stretching at 1731 cm^{-1}. This could be attributed to the carbonyl present on both, TPGS and PCL [35]. Also, we observed an overlapping of the C—H stretching band of PCL at 2942 cm^{-1} and that of TPGS at 2865 cm^{-1}. The absorption band at 3432 cm^{-1} is assigned to the terminal hydroxyl group, and the band at 1048 and 1192 cm^{-1} was due to the C—O stretching of PCL–TPGS copolymer.

3.2. Preparation and characterization of PTX-loaded nanoparticles

Nowadays, several methods are used to prepare polymeric NPs. In this work, we explored the preparation of PTX-loaded PCL–TPGS NPs using different methodologies as detailed above (Section 2.4). These techniques were compared to evaluate whether the preparation method could affect PTX loading, particle size, size distribution and surface charge. We compare these properties for the different NPs in Table 1. NPr-method was the first method used because is a simple, fast, reproducible and economic method that usually provides small size NPs. Also, we used the emulsion-solvent evaporation method because is the most widely employed technique to generate these systems [36]. In the case of NPr-method, we used acetone because it is miscible with the aqueous phase and solubilizes perfectly the amounts of PTX and PCL–TPGS used. Also, this organic solvent can be removed by evaporation under mechanical stirring over a short time [35]. In the case of US- and UT-method, we used DCM as organic solvent, because it is a very good solvent for the copolymer and drug used, and TPGS, as surfactant, because it is an excellent emulsifier that aligns at the oil–water interface to promote the stability of the particles by lowering the surface energy at low concentrations [34]. Preliminary assays (data not shown)

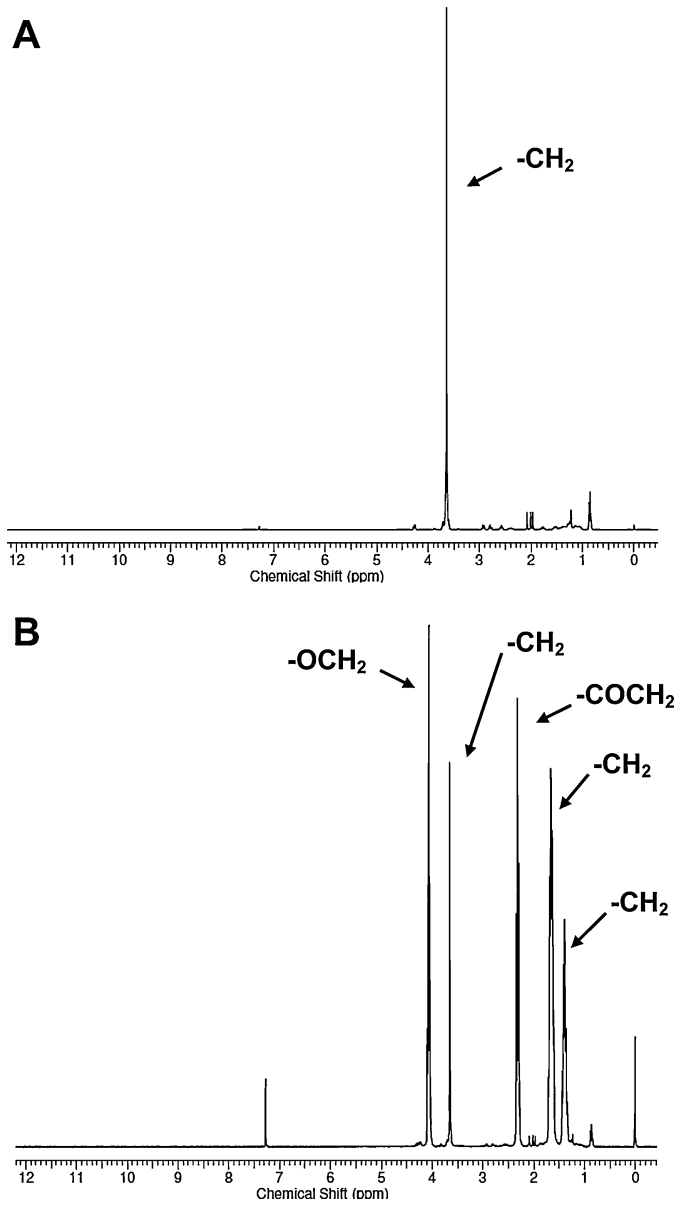

Fig. 1. ^{1}H NMR spectrum of TPGS (A) and PCL–TPGS (B) in $CDCl_3$.

indicate that 0.03% (w/v) is a suitable concentration to be used as stabilizer. This concentration concurs with previous observations [34,37].

The size and size distribution of the NPs is very important because smaller particles (<400 nm) tend to accumulate in the tumor sites due to the facilitated extravasation from the fenestrations in leaky vasculature [38]. NPr- and US-method produced smaller NPs (~260 and ~240 nm, respectively) compared to those produced by UT-method (~440 nm). All formulations prepared exhibit a unimodal particle size distribution, as also confirmed by the low values of polydispersity observed (Table 1). Zeta potential values were found between −30.0 and −37.8 mV. In all cases, we did not observe significant changes in the surface charge, independently of the preparation method. Negative zeta potential values of PCL–TPGS NPs may be due to the presence of ionized carboxyl groups of the PCL segments [39].

NPs prepared by NPr- and UT-method presented low values of DL (1.24 and 1.45% (w/w), respectively), while the particles produced by US-method 5.73% (w/w) (4.6 and 4.0-fold increase). Differences were not statistically significant ($p > 0.05$) for NPr- and UT-method; while between US- and UT-method, and US and NPr-method the differences were statistically significant ($p < 0.05$). The EE was much higher with the US-method (63.0%) than with the NPr- and UT-method (13.6 and 15.9%, respectively). Hence, PTX-loaded PCL–TPGS NPs prepared by US-method exhibited the smaller size and higher drug content. This is probably due to the higher energy released in the emulsification process by the ultrasonicator, leading to the formation of a more stable emulsion which was directly related to the size and drug loading of the NPs. Therefore, US-method was the most efficient preparation method used.

Surface morphology of the drug-loaded PCL–TPGS NPs was examined by SEM. The NPs prepared with the different techniques have a spherical shape and a smooth surface as shown in Fig. 2; in addition particle sizes were in good agreement with DLS data. In the microphotographs, drug crystals could not be visualized around the NPs or on the surface, suggesting that the drug was completely encapsulated.

3.3. Differential scanning calorimetry

DSC is one of the most frequent methods used to study the physicochemical interactions between drug and polymer in a formulation. This technique allows us to elucidate whether the drug is in crystalline or amorphous state. The present assay included NPs prepared by US-method because this formulation exhibited the highest drug loading percentage. PCL–TPGS presented an endothermic peak at 64.4 °C corresponding to copolymer melting. Blank NPs exhibited an endothermic event at 56.3 °C corresponding to PCL–TPGS melting. In this case, the nanoencapsulation procedure modified slightly the copolymer melting temperature. The physical mixture showed two endothermic peaks at 56.2 and 228.2 °C, corresponding to copolymer and PTX, respectively. The T_m of PTX in the physical mixture presented a slight deviation with respect to the T_m of the pure drug (219.5 °C); this peak was not observed in the PTX-loaded NPs suggesting the absence of crystalline drug in the NPs due to the process of encapsulation. Also PTX-loaded and blank NPs exhibit a similar endothermic peak (54.9 and 56.3 °C, respectively) corresponding to PCL–TPGS. This suggested that the addition of drug did not affect the copolymer structure.

3.4. In vitro PTX release

The *in vitro* cumulative release profiles of PTX encapsulated by NPr- and US-method are shown in Fig. 3. Both NP formulations exhibited a sustained release of PTX. It was clearly observed that the drug release was faster for NPr- than for US-method. The amount of drug released from the NPs in the first 24 h was ~20% and ~30% for

Table 1
Influence of the preparation method on the size, zeta potential, drug loading (DL) and encapsulation efficiency (EE) of PCL–TPGS NPs. Results are expressed as mean ± S.D. ($n = 3$).

Technique	Size (nm) (±S.D.)	PDI (±S.D.)	Zeta potential (mV) (±S.D.)	DL (% w/w) (±S.D.)	EE (%)
NPr-method	261.6 ± 9.5	0.15 ± 0.03	−30.0 ± 0.8	1.24 ± 0.06	13.6
UT-method	444.3 ± 21.7	0.20 ± 0.02	−37.8 ± 0.9	1.45 ± 0.16	15.9
US-method	237.8 ± 5.8	0.23 ± 0.01	−36.5 ± 1.1	5.73 ± 0.48	63.0

PDI, polydispersity.

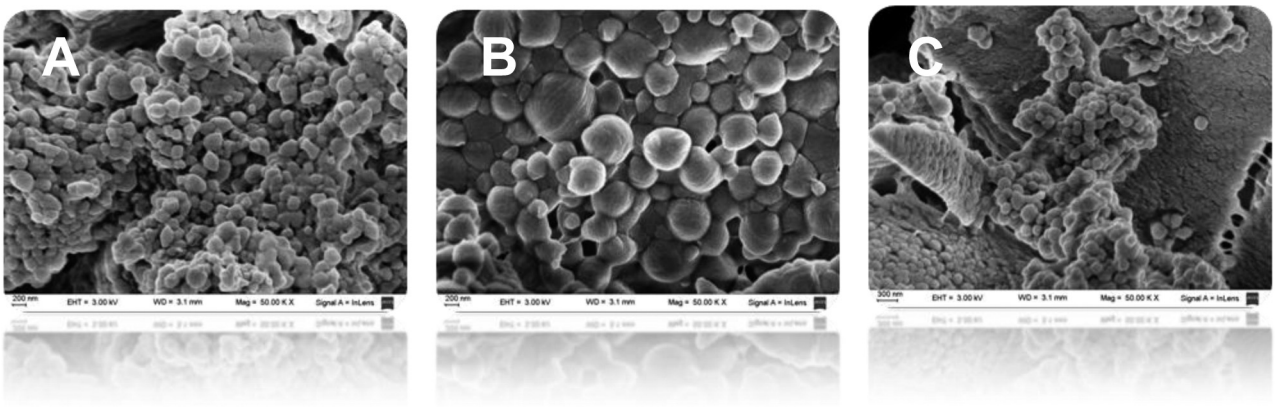

Fig. 2. SEM micrographs of PTX-loaded PCL–TPGS NPs prepared by NPr- (A), UT- (B) and US-method (C). Scale bar: 200 nm.

US- and NPr-method, respectively. After 96 h, the PTX release was ~45% for US-method and ~80% for NPr-method. Similar behavior was observed by Cheow et al. [40]. At 6 days, the entire drug load is completely released from the NPs prepared by NPr-method. The higher release of PTX from these NPs might be due to the dissolution and diffusion of the drug that was poorly entrapped in the polymer matrix. However, after the same period of 6 days, the other formulation released ~70% of drug. The slower and continuous release may be attributed to the diffusion of the drug localized in the PCL–TPGS core of the NPs prepared by US-method. These results clearly indicate that the release profile was influenced by the preparation technique. To predict the release kinetics, four drug release models (zero order, first order, Higuchi and Korsmeyer–Peppas) were used. When we use the first three models, the release profile of the NPs prepared by NPr-method was best fitted with the Higuchi model (R^2 adj = 0.993), while zero order model gave the best fit for NPs produced by US-method (R^2 adj = 0.997). Application of the Korsmeyer–Peppas model was performed to gain further insight into the mechanisms of release. In this case, the particles were considered as spheres [41]. For this geometric shape, n values of 0.43 indicate that the drug release is controlled by Fickian diffusion. Values of n between 0.43 and 0.85 indicate a mechanism known as anomalous transport (combination of drug diffusion and polymer chain relaxation as the solvent diffuse into the polymeric matrix). Finally, $n = 0.85$ indicates polymer relaxation [42]. The n values obtained were identical for both formulations ($n = 0.61$), suggesting that the mechanism of drug release could be a combination of drug diffusion, polymer chain relaxation and erosion. These results clearly indicate that: (i) the preparation technique governs the PTX release rate, and (ii) the copolymer, which forms the structure of NPs, determines the drug release mechanism.

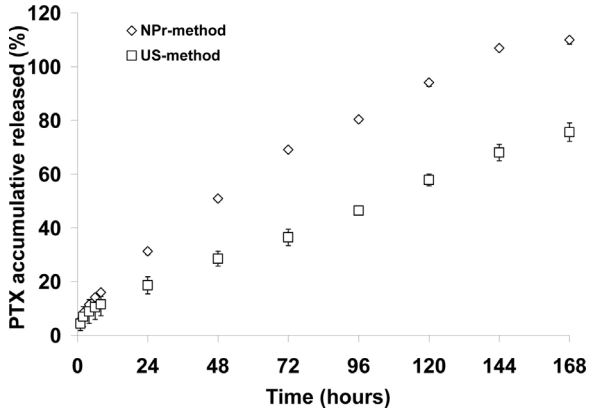

Fig. 3. *In vitro* drug release profiles from NPs prepared by NPr- and US-method over 168 h. Data are expressed as mean ± S.D. ($n = 3$).

3.5. *In vitro cytotoxicity*

The cytotoxicity of PTX-loaded PCL–TPGS NPs was tested in two different human breast cancer cell lines: an estrogen-dependent (MCF-7) and an estrogen independent (MDA-MB-231) using the WTS assay (Fig. 4). In the MCF-7 breast cancer cells, PTX-loaded NPs exhibited a significant higher cytotoxicity than PTX and commercial formulation Abraxane® at the concentrations used as percentage

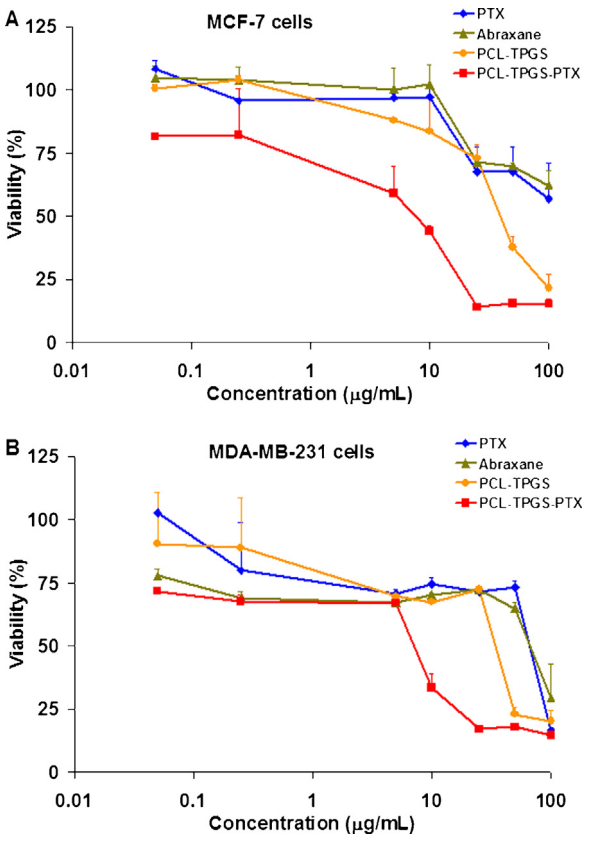

Fig. 4. Viability of human breast cancer MCF-7 and MDA-MB-231 cells determined by WST assay after incubation for 48 h with PTX-loaded PCL–TPGS NPs in comparison with PTX and Abraxane® at the same PTX dose and molar equivalent of blank PCL–TPGS NPs. (A) Viability of MCF-7 cells and (B) viability of MDA-MB-231 cells incubated for 48 h. Results are expressed as mean ± S.D. ($n = 3$). This experiment has been replicated at least twice for each cell line.

Table 2
IC_{50} values in MCF-7 and MDA-MB-231 cells after 48 h treatment by PTX, Abraxane®, and PTX-loaded NPs. Results are expressed as mean ± S.D. ($n = 3$).

Cell line	IC_{50} (μg/mL)		
	PTX	Abraxane®	PTX-loaded NPs
MCF-7	>100	>100	9.4 ± 2.3
MDA-MB-231	58.7 ± 2.4	67.9 ± 22.3	8.7 ± 1.1[a,b]

Note: Multiple comparisons were performed using one-way ANOVA with Tukey *post hoc* test ($n = 3$ experiments).
[a] Significant difference compared to PTX ($p < 0.01$).
[b] Significant difference compared to Abraxane® ($p < 0.01$).

of viability measured by WST assay (Fig. 4A). Also, it is important to remark that blank NPs displayed increasing cytotoxicity at the concentrations used in this study. The higher cytotoxicity of PTX-loaded NPs might be attributed to the combined effect of drug encapsulation and the selective chemotherapeutic effect of TPGS [26,43–45]. The other breast cancer cell line assayed was the MDA-MB-231. It is known as the triple-negative cell line because these cells lack the estrogen, progesterone and human epidermal growth factor type 2 receptors. Also, it is highly proliferative and aggressive. Tumors of this aggressive subtype have a poor overall prognosis [46]. Again, in our viability assay PTX-loaded NPs presented the most significant cytotoxicity profile against MDA-MB-231 cells compared to all the other formulations tested (Fig. 4B). Also, blank NPs showed cytotoxicity in MDA-MB-231 cells with increasing copolymer concentrations, as it was observed in the MCF-7 cells. For the two cell lines, the drug concentration played a major role in the *in vitro* cytotoxicity of the drug; higher PTX concentration resulted in higher cell mortality (Fig. 4A and B).

An important parameter for evaluate quantitatively the *in vitro* therapeutic effects of an anticancer drug is the IC_{50}, which represents the drug concentration needed to kill 50% of the cancer cells at a designated time. Table 2 shows the IC_{50} values of PTX, Abraxane® and PTX-loaded NPs in MCF-7 and MDA-MB-231 cells after 48 h incubation. In the MCF-7 cells, PTX-loaded NPs showed an estimated IC_{50} value of 9.4 μg/mL. In case of PTX and Abraxane®, their IC_{50} values could not be determined in this assay because at the higher concentration used (100 μg/mL) the viability was greater than 50%. Therefore we considered that PTX-loaded NPs were more effective (>10-fold) than PTX and Abraxane®.

It is important to note that in the triple negative MDA-MB-231 cell line, PTX-loaded NPs showed an IC_{50} value of 8.7 μg/mL, being more than six and seven-fold more effective than PTX and Abraxane®, respectively (Table 2). The data show clearly the advantage of our novel NPs *versus* PTX and the commercial formulation Abraxane®.

In addition, these results are in good concordance with previously investigations where PTX-loaded NPs have better anti-cancer activity compared to Taxol® [47,48].

3.6. *In vivo* pharmacokinetic studies

The *in vivo* performance of PTX formulated in PCL–TPGS NPs was compared with two formulations currently available for clinical use: Taxol® and Abraxane®. Taxol® is the conventional market formulation and the second is a clinically approved nanoformulation demonstrating significant improvement over the first. For this reason, we believe it is very important for improving therapy with PTX, extend the benchmark comparison to Abraxane® in animals. In this assay, we evaluated the following pharmacokinetic parameters: area under the curve (AUC); plasma elimination half-life ($t½$), total body clearance (Cl) and volume of distribution at steady state (V_{ss}) using Wistar rats at a dose of 6 mg PTX/kg. These parameters of PTX were obtained by noncompartmental analysis of plasma concentrations at selected time points. The pharmacokinetic curves of the PTX plasma concentration *versus* time after i.v. administration are presented in Fig. 5. In this, we could see that PCL–TPGS NPs exhibited significant pharmacokinetic advantages *versus* Taxol® and Abraxane®. The Taxol® profile show how rapidly the drug was cleared from the plasma after bolus administration. At 6 h, its concentration falls from a peak (4420 ng/mL) to a level (18 ng/mL) below the minimum therapeutic effective level [49]. In the case of Abraxane®, we observed a similar profile until 4 h. Then, the drug concentration was slowly dropped down and it remained below the therapeutic window. Instead, PTX-loaded PCL–TPGS NPs presented a similar profile than Abraxane®, but in this case the drug concentration remained in the therapeutic window. The pharmacokinetic profile of the NPs showed a clear advantage over the other formulations.

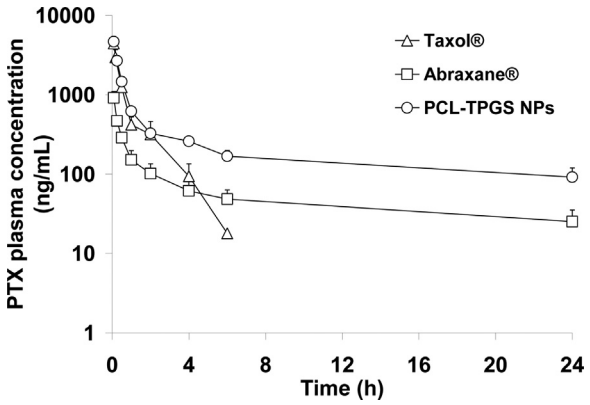

Fig. 5. Pharmacokinetic profile of Taxol®, Abraxane® and PTX-loaded PCL–TPGS NPs. Data are expressed as mean ± S.E. ($n = 5$).

Noncompartmental analysis of PTX plasma concentrations indicated that the encapsulation of PTX in NPs allows a rise of the $AUC_{0-\infty}$ to 7.07 μg/mL from 2.62 and 1.87 μg/mL for Taxol® and Abraxane®, respectively (Table 3) resulting in an increase of 270 and 378%, respectively. In addition, differences between NPs and Taxol®, and NPs and Abraxane® were statistically significant ($p < 0.05$). Also, we observed that the $t½$ of NPs (10.13 h) was prolonged by 11.64- and 1.22-fold compared to Taxol® and Abraxane®, respectively. In this case, we observed that the differences were statistically significant ($p < 0.05$) only between NPs and Taxol®, and Abraxane® and Taxol®. PTX-loaded PCL–TPGS NPs presented a low clearance rate when compared to Taxol®

Table 3
Pharmacokinetic parameters of PTX-loaded PCL–TPGS NPs compared with Taxol® and Abraxane®. Results are expressed as mean ± S.E. ($n = 5$).

Parameter	Units	Taxol®	Abraxane®	PCL–TPGS NPs
$AUC_{0-\infty}$	μg/mL h	2.62 ± 0.65	1.87 ± 0.38	7.07 ± 1.43[*,**]
$t½$	h	0.87 ± 0.23	8.25 ± 3.88[*]	10.13 ± 3.42[*]
Cl	mL/min	49.15 ± 12.90	58.10 ± 18.69	15.86 ± 2.29[*,**]
V_{ss}	L	2.13 ± 0.52	26.10 ± 9.16[*]	8.89 ± 1.88[*]

[*] $p < 0.05$ *vs.* Taxol®.
[**] $p < 0.05$ *vs.* Abraxane®.

and Abraxane® (Table 3). For this parameter, the differences were statistically significant ($p < 0.05$) between NPs and Taxol®, and NPs and Abraxane®. These results showed important pharmacokinetics advantages of the PTX-loaded PCL–TPGS NPs *versus* Taxol® and Abraxane®. Since PTX showed lower clearance and higher plasma AUC after administration of NPs compared with Taxol® and Abraxane®, it is expected that PTX-loaded PCL–TPGS NPs can increase the exposure of the tumoral cells to the taxane and extend its *in vivo* antitumoural activity [50]. Therefore, this would be a clear advantage over commercial formulations.

4. Conclusion

In this work, PCL–TPGS copolymer was successfully employed for the first time for the nanoencapsulation of PTX using three different methods. US-method resulted more effective than NPr- and UT-method to achieve particles with small size, uniform distribution and higher encapsulation efficiency. *In vitro* release assay indicates that PCL–TPGS NPs prepared by US-method released the drug more slowly than NPs prepared by NPr-method. These results showed that the US-method is advantageous to prepare a controlled release particulate system. *In vitro* studies showed that the PTX-loaded PCL–TPGS NPs prepared with the US-method presented better anticancer activity compared to PTX solution and the commercial formulation Abraxane® at different concentrations assayed on MCF-7 and MDA-MB-231 breast cancer cells. Also, PTX-loaded NPs showed better pharmacokinetic parameters in rats compared to Taxol® and Abraxane®. Based on these results, it can be concluded that our novel nanoparticles should be considered as an effective anti-cancer drug delivery system for chemotherapy.

Acknowledgements

Authors thank the University of Buenos Aires (Grant UBACyT 20020100300088 and 20020110200027), National Council for Scientific and Technological Research (CONICET) (Grant PIP 11420110100139), and the National Agency for Promotion of Science and Technology (ANPCyT) (Grant PICT-PRH 2008-00315). EB is supported by the PFDT fellowship from the ANPCyT (FONARSEC PICT-PRH 2008-00315), Argentina. GH, LG, CT and DAC are partially supported by CONICET, Argentina. Authors thank Dr. A. Montero Carcaboso for useful discussions.

References

[1] WHO – World Cancer Day – "Together it is possible". http://www.who.int/cancer/en/ (accessed January 2013).
[2] GLOBOCAN 2008 Estimated cancer Incidence, Mortality, Prevalence and Disability-adjusted life years (DALYs) Worldwide in 2008. http://globocan.iarc.fr (accessed January 2013).
[3] WHO – Breast cancer: prevention and control. http://www.who.int/cancer/detection/breastcancer/en/index.html (accessed January 2013).
[4] A. Gennari, P. Conte, R. Rosso, C. Orlandini, P. Bruzzi, Cancer 104 (2005) 1742.
[5] G. Ma, J. Yang, L. Zhang, C. Song, Anticancer Drugs 21 (2010) 261.
[6] A. Cirstoiu-Hapca, F. Buchegger, N. Lange, L. Bossy, R. Gurny, F. Delie, J. Control. Release 144 (2010) 324.
[7] A.K. Singla, A. Garg, D. Aggarwal, Int. J. Pharm. 235 (2002) 179.
[8] K. Yoncheva, P. Calleja, M. Agüeros, P. Petrov, I. Miladinova, C. Tsvetanov, J.M. Irache, Int. J. Pharm. 436 (2012) 258.
[9] S.-Ch. Lee, K.-M. Huh, J. Lee, Y.-W. Cho, R.E. Galinsky, K. Park, Biomacromolecules 8 (2007) 202.
[10] H. Gelderblom, J. Verweij, K. Nooter, A. Sparreboom, Eur. J. Cancer 37 (2001) 1590.
[11] S. Singh, A.K. Dash, Crit. Rev. Ther. Drug Carrier Syst. 26 (2009) 333.
[12] J.M. Meerum Terwogt, B. Nuijent, W.W. Ten Bokkel Huinink, J.H. Beijnen, Cancer Treat. Rev. 23 (1997) 87.
[13] H. Maeda, J. Wu, T. Sawa, Y. Matsumura, K. Hori, J. Control. Release 65 (2000) 271.
[14] P. Crosasso, M. Ceruti, P. Brusa, S. Arpicco, F. Dosio, L. Cattel, J. Control. Release 63 (2000) 19.
[15] T. Yang, F.-D. Cui, M.-K. Choi, J.-W. Cho, S.-J. Chung, C.-K. Shim, D.-D. Kim, Int. J. Pharm. 338 (2007) 317.
[16] R. Cavalli, O. Caputo, M.R. Gasco, Eur. J. Pharm. Sci. 10 (2000) 305.
[17] D.-B. Chen, T.-Z. Yang, W.-L. Lu, Q. Zhang, Chem. Pharm. Bull. 49 (2001) 1444.
[18] F. Danhier, N. Lecouturier, B. Vroman, C. Jérôme, J. Marchand-Brynaert, O. Feron, V. Préat, J. Control. Release 133 (2009) 11.
[19] Z. Wei, J. Hao, S. Yuan, Y. Li, W. Juan, X. Sha, X. Fang, Int. J. Pharm. 376 (2009) 176.
[20] W. Zhang, Y. Shi, Y. Chen, J. Hao, X. Sha, X. Fang, Biomaterials 32 (2011) 5934.
[21] I.-K. Park, Y.-J. Kim, T.-H. Tran, K.-M. Huh, Y.-K. Lee, Polymer 51 (2010) 3387.
[22] D. Yang, X. Liu, X. Jiang, Y. Liu, W. Ying, H. Wang, H. Bai, W.D. Taylor, Y. Wang, J.P. Clamme, E. Co, P. Chivukula, K.Y. Tsang, Y. Jin, L. Yu, J. Control. Release 161 (2012) 124.
[23] W.J. Gradishar, Expert Opin. Pharmacother. 7 (2006) 1041.
[24] A. Sparreboom, C.D. Scripture, V. Trieu, P.J. Williams, T. De, A. Yang, B. Beals, W.D. Figg, M. Hawkins, N. Desai, Clin. Cancer Res. 11 (2005) 4136.
[25] E. Bernabeu, D.A. Chiappetta, J. Biomater. Tissue Eng. 3 (2013) 122.
[26] H.J. Youk, E. Lee, M.K. Choi, Y.J. Lee, J.H. Chung, S.H. Kim, C.H. Lee, S.J. Lim, J. Control. Release 107 (2005) 43.
[27] A.M. Puga, A. Rey-Rico, B. Magariños, C. Alvarez-Lorenzo, A. Concheiro, Acta Biomater. 8 (2012) 1507.
[28] C.O. Kappe, Angew. Chem. Int. Ed. 43 (2004) 6250.
[29] Y.-J. Wang, C. Wang, C.-Y. Gong, Y.-J. Wang, G. Guo, F. Luo, Z.-Y. Qian, Int. J. Pharm. 434 (2012) 1.
[30] P. Costa, J.M. Sousa Lobo, Eur. J. Pharm. Sci. 13 (2001) 123.
[31] G. Schwach, M. Vert Int, J. Biol. Macromol. 25 (1999) 283.
[32] S.-S. Feng, L. Mei, P. Anitha, C.W. Gan, W. Zhou, Biomaterials 30 (2009) 3297.
[33] Z. Zhang, S.-S. Feng, Biomaterials 27 (2006) 262.
[34] Y. Ma, L. Huang, C. Song, X. Zeng, G. Liu, L. Mei, Polymer 51 (2010) 5952.
[35] M.A. Moretton, R.J. Glisoni, D.A. Chiappetta, A. Sosnik, Colloids Surf. B: Biointerfaces 79 (2010) 467.
[36] J. Prasad Rao, K.E. Geckeler, Prog. Polym. Sci. 36 (2011) 887.
[37] L. Mu, S.S. Feng, J. Control. Release 86 (2003) 33.
[38] F. Danhier, O. Feron, V. Préat, J. Control. Release 148 (2010) 135.
[39] F. Lince, D.L. Marchisio, A.A. Barresi, J. Colloid Interface Sci. 322 (2008) 505.
[40] W.S. Cheow, M.W. Chang, K. Hadinoto, Pharm. Res. 27 (2010) 1597.
[41] J. Siepmann, F. Siepmann, Int. J. Pharm. 364 (2008) 328.
[42] A. Debrassi, C. Bürger, C.A. Rodrigues, N. Nedelko, A. Ślawska-Waniewska, P. Dłużewski, K. Sobczak, J.M. Greneche, Acta Biomater. 7 (2011) 3078.
[43] C. Constantinou, A. Papas, A.I. Constantinou, Int. J. Cancer 123 (2008) 739.
[44] J. Neuzil, M. Tomasetti, Y. Zhao, L.-F. Dong, M. Birringer, X.-F. Wang, P. Low, K. Wu, B.A. Salvatore, S.J. Ralph, Mol. Pharmacol. 71 (2007) 1185.
[45] C.M. Neophytou, C. Constantinou, A.I. Constantinou, Cancer Res. 72 (Suppl. 1) (2012).
[46] C.R. Tate, L.V. Rhodes, H. Chris Segar, J.L. Driver, F. Nell Pounder, M.E. Burow, B.M. Collins-Burow, Breast Cancer Res. 14 (2012) R79.
[47] L. Zhao, S.-S. Feng, J. Pharm. Sci. 99 (2010) 3552.
[48] Z. Zhang, S.-S. Feng, Biomaterials 27 (2006) 4025.
[49] Y. Dong, S.-S. Feng, Biomaterials 28 (2007) 4154.
[50] T. Hamaguchi, Y. Matsumura, M. Suzuki, K. Shimizu, R. Goda, I. Nakamura, I. Nakatomi, M. Yokoyama, K. Kataoka, T. Kakizoe, Br. J. Cancer 92 (2005) 1240.